Exome sequencing implicates impaired GABA signaling and neuronal ion transport in trigeminal neuralgia

Weilai Dong[1]*, Sheng Chih Jin[1,2]*, August Allocco[3]*, Xue Zeng[1]*, Amar Sheth[3], Shreyas Panchagnula[3], Annie Castonguay[4], Louis-Étienne Lorenzo[4], Barira Islam[5], Geneviève Brindle[4], Karine Bachand[4], Jamie Hu[3], Agata Sularz[3], Jonathan Gaillard[3], Jungmin Choi[1,6], Ashely Dunbar[3], Carol Nelson-Williams[1], Emre Kiziltug[3], Charuta Gavankar Furey[3], Sierra Conine[3], Phan Q. Duy[3], Adam Kundishora[3], Erin Loring[1], Boyang Li[7], Qiongshi Lu[8], Geyu Zhou[7], Wei Liu[7], Xinyue Li[7], Michael C. Sierant[1], Shrikant Mane[9], Christopher Castaldi[9], Francesc López-Giráldez[9], James R. Knight[9], Raymond Sekula[10], Marc J. Simard[11], Emad N. Eskandar[12], Christopher Gottschalk[13], Jennifer Moliterno[3], Murat Günel [3], Jason L. Gerrard[3], Sulayman Dib-Hajj[14,15], Stephen G. Waxman[14,15], Fred G. Barker II[16,17,18], Seth L. Alper[19], Mohamed Chahine[20], Shozeb Haider[5], Yves De Koninck[20], Richard P. Lifton[1,2], and Kristopher T. Kahle[3,21,22,23,24]

[1]Department of Genetics, Yale School of Medicine, New Haven CT, USA.
[2]Laboratory of Human Genetics and Genomics, The Rockefeller University, New York, NY, USA
[3]Department of Neurosurgery, Yale School of Medicine, New Haven CT, USA.
[4]Centre de recherche de l'Institut universitaire en santé mentale de Québec (CRIUSMQ), Université Laval, Québec, Qc, Canada.
[5]University College London, School of Pharmacy, London, England.
[6]Department of Biomedical Sciences, Korea University College of Medicine, 02841 Seoul, Korea
[7]Department of Biostatistics, Yale School of Public Health, New Haven, Connecticut, USA.
[8]Department of Biostatistics & Medical Informatics, University of Wisconsin-Madison, Madison WI, USA.
[9]Yale Center for Genome Analysis, West Haven CT, USA.
[10]Department of Neurological Surgery, University of Pittsburgh School of Medicine and University of Pittsburgh Medical Center, Pittsburgh, PA, United States of America.
[11]Department of Neurosurgery, University of Maryland School of Medicine, Baltimore, MD , USA
[12]Department of Neurosurgery, Harvard Medical School and Massachusetts General Hospital, Boston, MA, United States.
[13]Headache Medicine, Yale Neuroscience Center, New Haven, CT, USA.
[14]Center for Neuroscience & Regeneration Research, VA Connecticut Healthcare System, West Haven, CT.
[15]Department of Neurology; Yale University, New Haven, CT.
[16]Harvard Medical School, Boston, Massachusetts, USA.
[17]Cancer Center, Massachusetts General Hospital, Boston, Massachusetts, USA.
[18]Department of Neurosurgery, Massachusetts General Hospital, Boston, Massachusetts, USA.
[19]Division of Nephrology and Center for Vascular Biology Research, Beth Israel Deaconess Medical Center; and Department of Medicine, Harvard Medical School, Boston, MA USA.
[20]Department of Psychiatry and Neuroscience, Université Laval, Quebec City, QC, Canada.
[21]Department of Pediatrics, Yale School of Medicine, New Haven CT, USA.
[22]Department of Cellular & Molecular Physiology, Yale School of Medicine, New Haven CT, USA.
*These authors contributed equally; [23]Senior author; [24]Lead contact

Correspondence:kristopher.kahle@yale.edu

ABSTRACT

Trigeminal neuralgia (TN) is a common, debilitating neuropathic face pain syndrome often resistant to therapy. The familial clustering of TN cases suggests genetic factors play a role in disease pathogenesis. However, no unbiased, large-scale genomic study of TN has been performed to date. Analysis of 290 exome-sequenced TN probands, including 20 multiplex kindreds and 70 parent-offspring trios, revealed enrichment in cases of rare, damaging variants in GABA receptor binding genes. Mice engineered with a novel, TN-associated *de novo* mutation (p.Cys188Trp) in the $GABA_A$ receptor Cl^- channel γ-1 subunit (*GABRG1*) exhibited trigeminal mechanical allodynia and striking face pain behavior. Other TN probands harbored rare, inherited or unphased damaging variants in Na^+ and Ca^+ channels, including a genome-wide significant variant burden in the α-1H subunit of the neuronal mechanosensory Ca^{2+} channel $Ca_V3.2$ (*CACNA1H*). These results provide the first genome-level insight into TN, and implicate genetically-encoded impairment of GABA signaling and neuronal ion transport in TN pathogenesis.

INTRODUCTION

Trigeminal neuralgia (TN), or "tic doulourex", is a severe neuropathic face pain syndrome characterized by recurrent, paroxysmal, lancinating face pain in the distribution of the trigeminal nerve that is variably triggered by sensory stimuli such as light touch or cold temperature[1]. TN affects ~3–4 per 100,000 people in the United States[2, 3]. The pathogenesis of "classical TN (cTN)" is frequently attributed to hyperexcitability of trigeminal ganglion neurons[4, 5, 6, 7] secondary to morphological compression of the trigeminal nerve root entry root by the cerebral vasculature (i.e., neurovascular compression [NVC])[8, 9, 10, 11, 12]. However, asymptomatic NVC has been noted in ~13-85% of asymptomatic subjects[13, 14, 15, 16]. Other cases of TN are related to trigeminal nerve infection (e.g., herpes zoster), trauma, demyelination (as in multiple sclerosis), or compression from a space-occupying lesion in the cerebello-pontine angle and are termed "secondary TN". However, a significant number of TN cases lack a demonstrable cause ("idiopathic TN [iTN]")[1, 17], including some cases with bilateral symptoms[18, 19].

First-line pharmacotherapy of TN includes the Na^+ channel blocker carbamazepine or its analogs[20], followed by other Na^+ channel- or GABA-modulating anticonvulsants such as gabapentin, lamotrigine, and topiramate[21]. The efficacy of these drugs suggests that neuronal hyperexcitability and aberrant ion transport may be involved in TN pathogenesis. For patients resistant to medical therapy, alternative interventional and surgical treatments are offered. These include neurolysis of the trigeminal ganglion and the cisternal segment of the nerve, as well as open neurosurgical microvascular decompression (MVD) of the nerve. However, the few reported randomized, placebo-controlled trials with long-term follow-up have left continued uncertainty about the efficacy of these medical and surgical interventions[22]. Gaps in our understanding of the cellular and molecular pathogenesis of TN have impeded the development of improved diagnostic, prognostic, and therapeutic measures.

The reported heritability of neuropathic pain conditions ranges from 16% to 50%[23, 24]. Familial forms of TN are well-documented, with many exhibiting autosomal dominant inheritance with incomplete penetrance[25, 26, 27, 28]. The average age of TN onset in familial forms is 44.4 years[26], nine years younger than the average age of sporadic TN cases[29]. A subset of familial forms demonstrates genetic anticipation, with progressively earlier disease onset across each succeeding generations[27, 30]. These observations implicate genetic determinants in TN pathogenesis. Previous studies using candidate gene approaches have identified an association of TN with a common single nucleotide polymorphism in the Na^+-dependent serotonin transporter SERT (*SLC6A4*)[31], and a gain-of-function *de novo* mutation (DNM) in the voltage-gated Na^+ channel Nav1.6 (*SCN8A*) in a single TN patient[32]. However, no large, unbiased, whole exome sequencing (WES) genomics study of TN has been performed to date.

The discovery of human genetic variants associated with TN could illuminate disease mechanisms, explain the variability of TN phenotypes and therapeutic responses, and identify potential drug targets for therapeutic intervention. Here, we present our analysis of WES of 290 exome-sequenced TN probands, including 20 multiplex kindreds and 70 parent-offspring trios. This approach, proven successful for several neurodevelopmental disorders[33, 34, 35, 36, 37], congenital heart disease[38, 39], and other heritable conditions[33, 40, 41], enables unbiased identification of rare, damaging DNMs and copy number variations (CNVs), along with rare, inherited single nucleotide

variants and insertions and deletions (indels) that contribute to disease pathogenesis. We hypothesized that rare, damaging variants in genes encoding proteins with important roles in the development, structure, or function of neurons in the peripheral or central trigeminal pain circuitry might confer risk for the development of TN.

RESULTS

We ascertained 290 probands with TN-related disorders, including 41 from the UK Biobank (**Table 1** and **Supplementary Table 1;** see **Methods**). UK Biobank patients included 34 probands (85.4%) (all singletons) with a primary diagnosis of TN (ICD10 code: G50.0), and 6 probands (17.1%) with atypical facial pain (ICD10 code: G50.1) and one proband with both. We recruited an additional 249 probands with either cTN, iTN type 1 (purely paroxysmal), or iTN type 2 (with concomitant continuous pain) that included 70 parent-offspring trios (see **Methods**). 63.9% (159/249) of probands had undergone neurosurgical intervention, including MVD (54.6%, 136/249), thermal or balloon rhizotomy (11.6%, 29/249), or gamma knife radiosurgery (14.9%, 37/249). 42.6% (58/136) of patients treated with MVD did not have sustained symptom relief. 19.1% (26/136) of these patients underwent a repeat MVD for post-operative recurrence of symptoms. Interestingly, 36/249 (14.5%) of cases were characterized by bilateral TN, and 41/249 (16.5%) of probands had a family history of TN.

To gain insight into the genomic architecture of TN, we first screened for rare, damaging heterozygous mutations (minor allele frequency [MAF] $\leq 1\times10^{-3}$ in Bravo[42]) in genes previously implicated in TN[31, 32]. Two probands each carried a deleterious missense (predicted as deleterious by metaSVM or have a CADD score ≥ 30[43, 44]; D-mis) mutation in non-conserved residues of *SCN8A*. p.Ile1583Thr maps to the ion transport domain, and p.Arg475Gln is located immediately adjacent to the voltage-gated Na^+ channel domain (**Supplementary Fig. 1**). No rare damaging mutations were identified in *SLC6A4*.

We next examined rare (MAF $\leq 5\times10^{-4}$), damaging (i.e., D-mis or loss-of-function [LoF]) variants that segregated with TN in 20 multiplex families with at least two affected individuals available for WES (**Fig. 1;** see **Methods**). Of the 10 genes with segregating variants in at least two families (**Supplementary Table 2**), only *SCN5A*, encoding Na^+ channel Nav1.5, was intolerant to both LoF (pLI ≥ 0.9) and missense variants (mis-z-score ≥ 2) (**Supplementary Fig. 2a**). In iTN-1 family TRGN201, *SCN5A* p.Arg1826His was shared by affected siblings TRGN201-1 and TRGN201-2. (**Supplementary Fig. 2b**). p.Arg1826His maps to a conserved residue in the Nav1.5 C-terminal cytoplasmic domain and is reported in ClinVar as pathogenic for long QT syndrome (**Supplementary Fig. 2c**). Nav1.5 Arg1826His-mediated Na^+ currents exhibit delayed inactivation and a 2- to 3-fold increase in late Na^+ current[45, 46]. *SCN5A* p.Phe1293Ser was shared by cTN-1 proband TRGN141-1 and her similarly affected maternal grandmother TRGN141-4 (**Supplementary Fig. 2a,b**). p.Phe1293Ser maps to *SCN5A* domain III and is predicted to alter Nav1.5 structure (**Supplementary Fig. 2c,d**). Of note, *SCN5A*-mutant TN patients did not report a history of cardiac arrhythmias or sudden death[47].

We also identified 4 rare CNVs (MAF $\leq 1x10^{-3}$) that segregated in 3 multiplex TN families (**Supplementary Table 3**). Among them, one ~500kb duplication covering the serine-threonine kinase *MAPK3* was shared by the proband and the affected mother, but not the unaffected father

in family TRGN190. *MAPK3* has been previously implicated in the pathogenesis of multiple trigeminal pain models[27, 48, 49, 50]. Interestingly, the TRGN190 proband with the *MAPK3* duplication was diagnosed with bilateral cTN-1 at 11 years of age and exhibited bilateral NVC on brain MRI. The patient was treated with bilateral MVD, followed one year later by repeat bilateral MVD for symptom recurrence. The proband's mother, also with a *MAPK3* duplication, was diagnosed with bilateral cTN-1 at 43 years of age. Though NVC was observed on her MRI, she declined surgery. Both patients reported significant symptom relief with the voltage-gated Na^+ channel blocker oxcarbazepine. The proband's sister was also diagnosed with oxcarbazepine-responsive unilateral iTN at 17 years of age, but was not available for WES.

We next examined the contribution of DNMs, including CNVs, to TN risk. Our TN cohort demonstrated a rate of 1.06 coding region DNMs per proband followed the expected Poisson distribution and closely matched the burden of DNMs in the control cohort (**Supplementary Fig. 3** and **Supplementary Table 4**). No genes contained more than one protein-altering DNM (**Supplementary Excel 1**). 11 *de novo* CNVs were identified, including a duplication in *KCNK1*, encoding the inward-rectifying K^+ channel TWIK1 (**Supplementary Table 5**). Of note, the pain insensitivity in multiple African rodents has been attributed in part to down-regulation of *kcnk1* expression[51]. No recurrent CNVs were observed.

We performed Gene Ontology (GO) enrichment analysis (see **Methods**)[52] of genes harboring damaging DNMs with high brain expression (above 75% percentile among all genes from murine RNA-seq[53]). Analysis showed the greatest enrichment among genes associated with the molecular function term "GABA receptor binding genes" (GO:0050811) (*GABRG1*, *TRAK1* [**Fig. 2a**]; enrichment >100, adjusted p-value = 5.85×10^{-3}). Damaging DNMs in GO:0050811 genes were enriched in TN cases but not controls (enrichment = 114.0, p-value = 1.5×10^{-4}) (**Supplementary Table 7**). Interestingly, several other notable genes with novel or rare damaging DNMs but not included under the GO term GO:0050811 term were identified that, similar to *GABRG1* and *TRAK1,* have elevated brain expression and play important roles in GABA signaling or neurotransmission. These include *ASTN2* (c.1736+2T>C)[54], *EEF2* (p.Arg839His)[55], *UNC80* (p.Lys2794*)[56, 57], and *KIF1B* (p.Arg928Trp)[58, 59, 60].

GABRG1 encodes the γ-1 subunit of the heteromeric ligand-gated gamma-aminobutyric acid type A receptor ($GABA_AR$) Cl^- channel. The γ-1 subunit is important in mediating the $GABA_AR$ response to benzodiazepines[61]. Patient TRGN124-1 with iTN-1 had a novel D-mis *GABRG1* DNM (p.Cys188Trp) in a conserved residue of the $GABA_AR$ γ-1 ligand binding domain that is predicted to disrupt a disulfide bond with Cys202 ($\Delta\Delta G$ = 3.8 kcal/mol) (**Fig. 2a-c**). Unrelated patient TRGN343-1 with iTN-2 carried the rare D-mis *GABRG1* mutation p.Tyr178His (MAF = 8.2×10^{-6}), which also maps to a conserved residue in the ligand binding domain and is predicted to disrupt a hydrogen bond between adjacent β-sheets ($\Delta\Delta G$ = 1.7 kcal/mol) (**Fig. 2a-c**). Another TN patient in the UK Biobank carried a rare stop-gain mutation in *GABRG1* (p.Trp53*) located just before the ligand-binding domain.

TRAK1 encodes a kinesin adaptor protein that that regulates the anterograde axonal transport of mitochondria and $GABA_ARs$[62]. Patient TRGN261-1 with iTN-2 had a novel D-mis *TRAK1* DNM (p.Glu798Lys) (**Fig. 2a**) in a conserved residue of the second kinesin-binding Milton domain of *TRAK1* (**Fig. 2b).** Unrelated patient TRGN107-1 with cTN-1 carried the unphased heterozygous

D-mis *TRAK1* mutation (p.Arg124Gln) with a MAF just above our threshold (1.6×10^{-5}). p.Arg124Gln maps to a highly conserved residue in the *TRAK1* HAP1_N domain (IPR006933) that directly participates in $GABA_AR$ trafficking in conjunction with kinesin (KIF) proteins[63]. Recessive *TRAK1* mutations cause early infantile epileptic encephalopathy (OMIM# 618201)[62] and *Trak1* knockout mice exhibit severely reduced CNS abundance of $GABA_ARs$[63].

A total of 9 rare (MAF $\leq 1.0\times10^{-5}$) damaging *de novo*, transmitted, or unphased mutations were identified in GO:0050811 GABA receptor binding genes, yielding enrichment compared to gnomAD controls (OR = 3.7, Fisher's exact p-value = 4.2×10^{-3}; **Supplementary Table 8, 9**). These genes included $GABA_AR$ subunit α-5 *GABRA5* and trafficking regulators *PLCL1*, *JAKMIP1* and *ARFGEF2*. Extension of our search to the 21 genes encoding HUGO Gene Nomenclature Committee (HGNC)-designated GABA receptor subunits identified two additional novel, damaging heterozygous mutations in the $GABA_AR$ α-6 and δ subunits, *GABRA6* and *GABRE* (**Supplementary Fig. 4a**). *GABRA5* p.Glu107Gln and *GABRA6* p.Glu90Ala both map to respective ligand-binding domains, whereas *GABRE* p.Trp300* affects the neurotransmitter gating domain (**Supplementary Fig. 4b-d**).

As proof-of-principle, we generated a mouse model of one of the newly identified human TN-associated $GABA_AR$ DNMs (*GABRG1* p.Cys188Trp), using Crispr/CAS9 mutagenesis (see **Methods**, **Supplementary Fig. 5**). To test for trigeminal pain hypersensitivity, we quantified nocifensive behaviors using a modified version of a facial stimulation test[64]. In contrast to wild-type littermates (n = 23 mice), mutant mice (n = 25) showed significant nocifensive behaviors in response to tactile stimulation of the trigeminal nerve region (**Fig. 2d;** see **Methods**; $p < 0.0001$; Mann-Whitney test; **Supplementary Video 1** and **Supplementary Excel 2**) in both males (n = 11 wild type *&* 12 mutants) and females (n = 12 wild type *&* 13 mutants), respectively (p-value=0.39 for females; p-value=9×10^{-4} for males; Kruskal-Wallis test). No significant difference in nocifensive behavior was observed between male and female mutants (p-value=0.40). To measure nociceptive withdrawal threshold, we also used a modified mechanical threshold test[65, 66]. Mutant mice (n = 11) showed a significantly lower nociceptive withdrawal threshold than wild-types (n = 9; p-value = $1.0\text{x}10^{-3}$; Mann-Whitney test **Fig. 2e** and **Supplementary Excel 3**). Hind paw nociceptive withdrawal threshold was also significantly reduced in mutant mice (p-value= $1.6\text{x}10^{-3}$; **Fig. 2f** and **Supplementary Excel 3**).

Next, we performed burden analysis of rare *de novo* and inherited/unphased variants in 290 TN probands, adjusting for *de novo* mutability using a one-tailed binomial test (see **Methods**). Analysis of ultra-rare variants at MAF $\leq 1\times10^{-5}$ did not identify significantly enriched genes. However, among moderately rare variants at MAF $\leq 1\times10^{-4}$, the Cav3.2 T-type Ca^{2+} channel α-1H subunit (*CACNA1H*) reached genome-wide significant enrichment in cases (3.7, p-value=2.4×10^{-6}; **Fig. 3a** and **Supplementary Table 10a**). *CACNA1H* contained 19 predicted damaging variants, including one LoF variant and 18 D-mis variants (**Supplementary Table 10b**). Among these, 16 are unphased, and 3 are transmitted with incomplete penetrance. The *CACNA1H* variants map to extracellular, intracellular and intra-membrane regions of the ion channel (**Fig. 3b**) and are predicted to impact Cav3.2 protein structure **(Supplementary Fig. 6**). In one family, the *CACNA1H* D-mis variant p.Arg1674His was shared by proband TRGN282-1 and his sister TRGN282-2, both similarly affected by medically-intractable iTN1.

Last, we examined recessive genotypes. No genes harbored more than 1 recessive genotype in 249 TN probands (see **Methods**). However, case-control analysis comparing rare damaging hemizygous variants (MAF $\leq 5\times10^{-5}$) in 49 male TN probands to male controls in gnomAD identified *CACNA1F*, encoding the Cav3.2 T-type Ca^{2+} channel α-1H subunit, as the most significantly enriched gene (OR=14.2, p-value = 1.56×10^{-3}; **Supplementary Table 11a**). *CACNA1F* contained three rare D-mis variants (**Fig. 3c** and **Supplementary Table 11b**). p.Ala1335Thr and pArg1289Gly respectively mapped to the exofacial and endofacial surfaces of the channel. p.Ile721Val mapped to an extracellular loop of the channel. All three variants are predicted to significantly impact *CACNA1F* channel structure (**Supplementary Fig. 7**).

DISCUSSION

These results provide the first insight into the genomic architecture of TN. We ascertained the largest collection of familial forms of TN to date, and identified several candidate genes with mutational enrichment in TN probands. Our findings implicate *de novo* and inherited rare, damaging variants in GABA signaling and other ion transport genes in TN pathogenesis in a subset of patients. Our creation of a novel knock-in mouse with the TN-associated *de novo GABRG1* p.Cys188Trp mutation represents, to our knowledge, the first TN animal model engineered with a human mutation.

Previous candidate gene sequencing approaches had identified *SCN8A* and *SLC6A4* as potential TN-associated genes[31, 32]. In our WES study, we detected only two rare transmitted mutations in *SCN8A* and none in *SLC6A4*. Nonetheless, our data implicate other ion transport pathways in the genetic architecture of TN, including genes related to the function of the ligand-gated $GABA_AR$ Cl^- channel. These findings are consistent with the expression of $GABA_ARs$ along sensory axons[67, 68], with the well-documented role of $GABA_AR$ signaling in trigeminal pathway nociception[46, 69, 70, 71, 72], with the efficacy of GABA-modulating drugs in some TN patients[73, 74] (**Supplementary Table 12**), and with the established importance of $GABA_AR$ disinhibition and consequent neuronal hyperexcitability in neuropathic pain[69, 70, 71]. These observations support our speculation that the not infrequent co-occurrence of anxiety, depression, and other psychiatric conditions with TN, especially those in younger patients[75] (often unresponsive to MVD[13]), may reflect pleiotropy of germline variants impacting other aspects of GABA signaling.

In addition to variants in GABA signaling genes, we also identified dominant variants in the *SCN8A*-related Nav1.5 Na^+ channel gene *SCN5A* in two multiplex TN families; a genome-wide significant enrichment of dominant variants in the $Ca_v3.2$ α-1H subunit *CACNA1H*; and multiple X-linked hemizygous variants in the related $Ca_v3.2$ α-1F subunit *CACNA1F*. *SCN5A* mutations are well known to cause cardiac rhythm disorders including long QT syndrome subtype 3, Brugada syndrome, and cardiac conduction disease[76], but are also expressed in the brain[77] and have been implicated in both epilepsy[78] and schizophrenia[47]. *CACNA1H* variants has been previously implicated in congenital pain[79] and epilepsy[80]. T-type Ca^{2+} currents mediated by $Ca_v3.2$/α-1H are responsible for the excitatory effects of GABA in sensory neurons[81] and mechanosensation in nerve root ganglia[82]. Increased expression of $Ca_v3.2$ in damaged dorsal root ganglion neurons contributes to the development of neuropathic pain triggered by spared nerve injury[83]. The closely-related $Ca_v3.1$ has been shown to be a key element in the pathophysiology of a mouse model of trigeminal neuropathic pain[84]. Mechanical thresholds of pain are significantly altered in a rat model of congenital stationary night blindness with a *Cacna1f* mutation[85]. Detailed electrophysiology of

these TN-associated *SCN5A*, *CACNA1H*, and *CACNA1F* channel variants in cell culture systems and animal models will be rich topics for future investigation.

How might these mutations and other gene variants contribute to TN pathology? One possibility is a "genetic-mechanical" model, in which a germline mutation confers increased sensitivity of the trigeminal ganglia or axons to neurovascular compression (NVC) by an offending blood vessel, such as the superior cerebellar artery in the cerebello-pontine angle. This mechanism may contribute to unilaterality of symptoms in some patients with NVC, and has been proposed for a gain-of-function mutation in *SCN8A*[32]. A germline mutation could also predispose patients to the development of bilateral symptoms, as is seen in some TN patients. Alternatively, a germline mutation could predispose an individual to later-onset TN arising from a second somatic mutation in the other allele of the same, or another gene, in trigeminal ganglion neurons or other downstream brainstem or thalamo-cortical neurons in the trigeminal system circuitry. Such a "two-hit" model has been seen in other neurovascular cutaneous syndromes with unilateral or multifocal lesions[86, 87, 88].

Given the role of common variants in multiple neuropathic pain disorders[89, 90, 91], we also examined the contribution to TN from common variants through a genome-wide association analysis of 236 European cases and 348,048 ethnicity-matching controls from the UK Biobank. No common variants reached genome-wide significance (**Supplementary Fig. 8**). However, the small number of available cases limited the power of our analysis. A power calculation suggests that more than 3,500 cases are needed to achieve 80% power assuming moderate effect size (λ=1.4) and a minor allele frequency of 0.2 for risk alleles (**Supplementary Fig. 9**). Thus, future studies examining common variants will require greater numbers of patients. Although childhood and adolescent onset of TN has been reported[92], the high prevalence of TN and its inconsistent segregation patterns within families suggest that complex epistatic interactions, gene-environment interactions, or effects from common polygenic variants could also play important pathogenic roles in TN[89, 93].

Our data suggests rare, damaging exonic variants likely contribute to the pathogenesis of a small fraction of TN cases. Nonetheless, continued gene discovery and functional analysis of these variants, including mechanistic work and drug screening in humanized animal models such as our *GABRG1* p.Cys188Trp knock-in mouse, could further elucidate TN pathophysiology, improve diagnostics, and optimally stratify certain patients for specific treatments (e.g., a GABA-modulating drug instead of a craniotomy for MVD). Our findings suggest a WES approach might also be suitable to study of hemifacial spasm, another cranial nerve pain syndrome with known familial occurrences that has been classically attributed to NVC and treated with neurosurgical MVD[94, 95, 96, 97, 98, 99, 100]. Moreover, the identification of novel mutations (even in single patients) has the potential to identify unexpected, new targets for development of non-addictive analgesics[101]. Overall, these considerations provide impetus for WES of additional TN case-parent trios, and for the functional study of discovered variants.

METHODS

Case cohort, enrollment, phenotyping, and exclusion criteria

We recruited 249 probands with TN, including 70 trios and 20 multiplex kindreds with two or more affected individuals among first or second-degree relatives. Inclusion criteria included male or female patients meeting the diagnostic criteria specified in ICHD-3 for either classical trigeminal neuralgia (13.1.1.1) or idiopathic trigeminal neuralgia (13.1.1.3)[102]. Participants were further subdivided into either "13.1.1.1.1 Classical TN, purely paroxysmal" ("cTN-1") and "13.1.1.1.2 Classical TN with concomitant continuous pain" ("cTN-2"), or "13.1.1.3.1 Idiopathic TN, purely paroxysmal" ("iTN-1") and "13.1.1.3.2 Idiopathic TN with concomitant continuous pain" ("iTN-1"), according to ICHD-3 criteria[102]. By definition, "13.1.1.2 Secondary TN", including "13.1.1.2.1 TN attributed to multiple sclerosis", "13.1.1.2.2 TN attributed to space-occupying lesion", "13.1.1.2.3 TN attributed to other cause", and "13.1.2 Painful trigeminal neuropathy" related to previous trauma, surgery, or radiation to the trigeminal nerve ipsilateral to pain were excluded from analysis. Also excluded were patients with psychiatric or mental illness that might interfere with patients' ability to grant informed consent or to complete clinical questionnaires. Diagnoses were assigned after full review of each patient's medical history and a neurological examination by a neurologist and neurosurgeon, along with a review of each patient's brain MRI by a neuroradiologist. Patients and participating family members additionally provided buccal swab samples (Isohelix SK-2S DNA buccal swab kits), medical records, radiological imaging studies and official written reports, neurosurgery operative reports, and TN phenotype data. Written informed consent for genetic studies was obtained from all participants. Parent or legal guardian authorization was obtained in writing for sample collection of all minors in this study. All study protocols were approved by the Yale Human Research Protection Program and Institutional Review Board.

Control cohorts

Controls consisted of 1,798 previously analyzed families with one offspring with autism, one unaffected sibling, and unaffected parents. In this study only the unaffected sibling and parents were analyzed. Controls were designated as unaffected by SSC[103]. Permission to access SCC genomic data in the National Institute of Mental Health Data Repository was obtained. Written informed consent for all participants was provided by the Simons Foundation Autism Research Initiative.

Exome sequencing

70 trios and 179 singletons were sequenced at the Yale Center for Genome Analysis following the same protocol. Briefly, genomic DNA from venous blood or saliva was captured using the Nimblegen SeqxCap EZ MedExome Target Enrichment Kit (Roche) or the xGEN Exome Research Panel v1.0 (IDT) followed by Illumina DNA sequencing as previously described[39]. At each site sequence reads were independently mapped to the reference genome (GRCh37) with BWA-MEM and further processed using GATK Best Practices workflows[104, 105, 106] including duplication marking, indel realignment, and base quality recalibration, as previously described[107]. Single nucleotide variants and small indels were called using GATK HaplotypeCaller and

Freebayes[108] and annotated using ANNOVAR[109], dbSNP (v138), 1000 Genomes (August 2015)[106], NHLBI Exome Variant Server (EVS; https://evs.gs.washington.edu/EVS/)[110], ExAC (v3)[111] and Bravo[112]. The MetaSVM and the Combined Annotation Dependent Deletion (CADD) algorithms were used to predict deleteriousness of missense variants ("D-mis", defined as MetaSVM-deleterious or CADD ≥30)[43, 44]. Candidate variant calls were validated using Sanger sequencing.

Kinship analysis and removal of duplicated samples

Pedigree information and participant relationships were confirmed using pairwise PLINK identity-by-descent (IBD) calculation[113] and pairwise comparison of high quality ultra-rare SNPs absent from public databases (ExAC and gnomAD)[114]. Individuals with ≥ 90% IBD or shared ultra-rare SNPs were identified as sample duplicates and removed from analysis.

Principal component analysis

EIGENSTAT software[115] was used to classify ethnicities through analyzing tag SNPs in cases and HapMap samples with known ethnicities. Principal component analysis was then performed to cluster the studied samples with HapMap samples using R software (version 3.4.1)[116], and the ethnicities of the cases were determined based on their best clustered ethnicity group against HapMap populations.

Variant filtering

DNMs were called using TrioDenovo[117] as described previously[107] and filtered using stringent hard cutoffs including: (1) in-cohort allele frequency $\leq 4 \times 10^{-4}$ for controls and MAF $\leq 4 \times 10^{-4}$ across all samples in 1000 Genomes, EVS, and ExAC, Bravo for cases due to limited cohort size, (2) a minimum of 10 total reads total, 5 alternative allele reads, and a minimum of 20% alternate allele ratio in the proband for alternate allele reads ≥ 10 or ,for alternate allele reads < 10, a minimum 28% alternate ratio, (3) a minimum depth of 10 reference reads and alternate allele ratio < 3.5% in parents, and (4) exonic or canonical splice-site variants.

For transmitted heterozygous variants, we filtered for high-quality heterozygotes (pass GATK Variant Score Quality Recalibration [VQSR], minimum 8 total reads, and genotype quality [GQ] score ≥ 20)[106, 111]. Variants with large impact on protein structures including LoF (canonical splice-site, frameshift insertion/deletion, stop-gain, stop-loss) and D-mis variants were considered for the analysis. Common variants with MAF > 5×10^{-3} within the cohort were excluded. Both rare (MAF ≤ 1×10^{-5} in Bravo) and moderately rare (MAF ≤ 1×10^{-4} in Bravo) variants were tested for enrichment across all genes of the genome.

We filtered recessive variants for rare (MAF ≤ 10^{-3} in Bravo and in-cohort MAF ≤ 5×10^{-3}) homozygous and compound heterozygous variants that exhibited high quality sequence reads (pass GATK VSQR, have ≥ 4 total reads for homozygous and ≥ 8 reads for compound heterozygous variants, have a GQ ≥ 10 for homozygous and GQ ≥ 20 for compound heterozygous variants). Only LoF, D-mis, and non-frameshift indels were considered potentially damaging to the disease.

Hemizygous variants were filtered by the same criteria as were recessive variants except for a more stringent frequency filter (MAF $\leq 5\times10^{-5}$ in Bravo and in-cohort MAF $\leq 5\times10^{-3}$).

Segregated variants in familial cases were filtered for rare (MAF $\leq 5\times10^{-4}$ in Bravo and in-cohort MAF $\leq 5\times10^{-3}$) and damaging (LoF and D-mis) dominant variants shared by affected individuals but not found in unrelated individuals.

Finally, *in silico* visualization was performed on all *de novo*, heterozygous, recessive variants, and hemizygous variants that (1) appeared at least twice or (2) were among the top 20 significant genes from the burden analysis, or (3) segregated in the families. Sanger validation was performed on candidate variants of interest.

De novo enrichment analysis

The expected number of DNM per gene per variant class was obtained based on a mutation model developed previously[118]. A one-tail Poisson test was used to compare the observed number of DNMs across each variant class to the expected number under the null hypothesis. The R package 'denovolyzeR'[107] was used to perform all *de novo* analyses.

Gene Ontology Enrichment Analysis

Functional profiling of 10 genes with high brain expression (brain expression rank $\geq$ 75%)[53] harboring DNMs was conducted with g:GOSt from g:Profiler[119], a tool that performs gene set overrepresentation/enrichment analysis and detects statistically enriched terms from functional information sources, including the Gene Ontology database[120, 121]. We used all annotated genes as the statistical domain scope, the g:SCS algorithm[119] to address multiple testing, and $p = 0.05$ as a user-defined threshold for statistical significance.

Case-control burden analysis

Case and control cohorts were processed using the same pipeline and filtered with the same criteria as described (see **Variant filtering** in **Methods**). A one-sided Fisher's exact test was used to compare the observed number of mutations in each variant class examined in cases to the same variant class in controls under the null hypothesis. The gnomAD controls we used are without TOPMed samples.

Copy number variation analysis

To identify CNVs from WES data, the aligned reads were imported into XHMM (eXome-Hidden Markov Model)[122]. Potential CNVs were inspected visually and prioritized based on Phred-scaled quality score, genomic length, GC content of targets, and low sequence complexity.

Protein structural modelling

The sequence of human SCN5A protein was downloaded from UniProt (Q14524) and aligned with the cryo-electron microscopy structure of the human Nav1.2-beta2-KIIIA (PDB id: 6J8E,

resolution: 3.00 Å) in ICM-Molsoft[123, 124] (**Supplementary Fig. 10**). The homology model was built in ICM-Molsoft based on an 80% sequence identity over resolved residues of human Nav1.2-beta2-KIIIA complex.

The sequence of human CACNA1H protein was downloaded from UniProt (O95180). The structures of the human Cav3.1 (PDB id: 6KZO, resolution 3.3 Å) and rabbit Cav1.1 complex (PDB id: 5GJW, resolution: 3.6 Å) were used to model the protein using homology tool of ICM-Pro[125, 126] (**Supplementary Fig. 11**). The initial model was built based on an 85% sequence identity over the resolved residues of human Cav3.1. As the homologous sequence for the loop harbouring residue of interest (R1674) and the surrounding region between 1562-1619 residues were missing in the structure of human Cav3.1, it was built using rabbit Cav1.1 as the template.

The sequence of human CACNA1F protein was downloaded from UniProt (O60840) and aligned with the cryo-electron microscopy structure of the rabbit Cav1.1 complex (PDB id: 5GJV, resolution: 3.6 Å) in MolSoft ICM-Pro ver 1.8.7c[125, 127] (**Supplementary Fig. 12**). The homology model was built in ICM-Pro based on a 75% sequence identity over the resolved residues of rabbit Cav1.1 complex. All the investigated residues lie in the conserved region of the protein.

The sequence for human Gamma-Aminobutyric Acid Type A Receptor Gamma1 Subunit (GABRG1) was obtained from UNIPROT as accession number Q8N1C3. The protein modelling protocol was identical was for the three proteins. The downloaded Protein Data Bank structure (PDB id 6D6U) was used as a template to construct homology models using MODELLER[128] (**Supplementary Fig. 13**).

Twenty models were subjected to restrained energy minimization to relieve steric clashes between or among side chains. Stereochemical parameters were analyzed using PROCHECK[129] and PROSA[130]. The final model was chosen based on a combination of the lowest energy function score (Dope) within the modeling program and model satisfaction of standard PROCHECK and PROSA criteria. Mutations were constructed and change of *in silico* free energy (ΔΔG) was calculated using the ICM mutagenesis program (www.molsoft.com)[127]:

$$\Delta\Delta G = \Delta G_{misfolded} - \Delta G_{unfolded}$$

$\Delta G_{unfolded}$ refers to the sum of the energies attributed to the individual residues before the mutation, while $\Delta G_{misfolded}$ refers to the sum of the energies attributed to the individual residues after the mutation. A positive ΔΔG is proportional to the magnitude of the predicted destabilization effect on the protein caused by the point mutation.

Enrichment analysis for the dominant variants

A one-sided binomial test was performed to compare the observed number of damaging dominant variants within each gene with the expected number as described before[38], and calculated using the following formula:

$$Expected\ Counts_i = N \times \frac{Mutability}{\sum_{Genes} Mutability}$$

where 'i' denotes the 'i^{th}' gene; 'N' denotes the total number of damaging dominant variants; Mutability refers to the *de novo* probability in each gene. The p-value threshold after Bonferroni multiple testing correction is 2.6×10^{-6} (0.05/19,347).

Gabrg1 mouse model and pain testing

The *Gabrg1* knock-in mouse model was generated using CRISPR/Cas9 as described[131, 132]. In brief, a T7-sgRNA template was prepared by PCR[131], incorporating the antisense guide sequence TAGGAAAATTATGAAGTTGA (from the mouse *Gabrg1* gene target region) and then used for in vitro transcription and purification with the MEGAshortscript T7 Transcription Kit and MEGAclear Transcription Clean-Up Kit, respectively (both from Thermo Fisher Scientific). Cas9 mRNA (CleanCap, 5moU-modified) was purchased from TriLink Biotechnologies and the homology-directed repair (HDR) oligonucleotide (142 b including 65 b homology flanks was ordered from Integrated DNA Technologies as a phosphorothioate-protected Ultramer. All animal procedures were performed according to NIH guidelines and approved by the Yale IACUC. C57BL6/N strain mice were obtained from Charles River and cytoplasmic microinjections of the sgRNA, Cas9 mRNA and HDR oligo into single-cell embryos were performed by the Yale Genome Editing Center. DNA lysates of tissue biopsies from potential founder pups were screened by PCR amplification with the following primers (F5′- AGGAGGTCCAAATGCTGTT and R5′- GGGAAGGGCGGTAGATG), followed by diagnostic PstI digestion and sequencing confirmation.

Pain hypersensitivity was measured using complementary approaches. Nociceptive withdrawal thresholds of the hind paw and trigeminal nerve region were quantified using the Simplified Up-Down method (SUDO)[65, 66]. The experimental group consisted of male and female mice carrying C188W mutations in *Gabrg1*. Sex-matched WT mice were included in the control group. Mice were placed in a transparent Plexiglas cage atop a wire mesh and were free to move about. After 60 minutes of acclimation, withdrawal responses were assessed. To assess sensitivity in the trigeminal nerve regions, Von Frey filaments (Stoelting, USA) were applied perpendicularly to the region of interest. A positive reaction was noted if the animal exhibited a vigorous head retraction or rapid grooming of the muzzle region. The entire SUDO procedure was repeated twice per animal for each nerve region at 5 months of age. A Mann-Whitney test was performed to assess statistical significance of differences between groups. To assess, nocifensive behavior to stimulation of the trigeminal area we also used a complementary modified version of a facial stimulation test[64]. Mice were stimulated once using filament #7 (0.6 g) and the subsequent grooming response was video recorded. Positive (presence of a stimulus-associated grooming response) and negative responses (absence of grooming behavior) were scored as values of +1 or -1 value, respectively. Mice were tested 3 times, on different days. Analysis of the videos was assessed by an experimenter blind to the animal's genotype.

Genome-wide association analysis

Imputed genotype array data of 48,7395 samples were obtained from UK Biobank. Only SNPs which have a MAF>0.05, have a missing genotype rate < 0.01 and passed the Hardy-Weinberg test (H-W p-value >0.001) were considered for the analysis using plink[133]. Subjects with self-report and genetically confirmed European ancestry were included (UK Biobank data filed 22006),

whereas related subjects (relatedness > 0.1 by gcta64[134]) were excluded. These filters yielded in 236 cases with TN (ICD10 code: G50.0 or G50.1) and 348,048 controls. A Multivariate Logistic Regression was performed using plink[133]. The covariates included gender and the top 10 principle components. The Manhattan plot was generated using the R (3.4.1) package qqman.

ACKNOWLEDGMENTS

We thank the patients and families who participated in this research. We acknowledge support from the Yale-NIH Center for Mendelian Genomics (5U54HG006504) and an NIH NRCDP award to K.T.K and a Canadian Institute of Health Research (CIHR) Foundation grant (FDN389050) to Y.D.K. This research has been conducted using the UK Biobank Resource under Application Number 29900. W.D. was supported by American Heart Association Predoctoral Fellowship. S.C.J. was supported by the James Hudson Brown-Alexander Brown Coxe Postdoctoral Fellowship, the American Heart Association Postdoctoral Fellowship (18POST34060008), and the K99/R00 Pathway to Independence Award (K99HL143036 and R00HL143036-02). Y.D.K. was supported by a Canada Research Chair in Chronic Pain and Related Brain Disorders.

FIGURE LEGENDS

Figure 1. Pedigrees for 20 TN familial cases. 20 familial cases with ≥ 2 members available for whole-exome sequencing (WES) are shown with sample IDs. Black circle/squares: Subjects with TN diagnosis.

Figure 2. Damaging *de novo* and inherited mutations in *GABRG1* and *TRAK1* in TN probands. (a) *De novo* and inherited mutations in *GABRG1* and *TRAK1*. Pedigrees with Sanger-validated mutant bases marked on the chromatograms. (b) Mapping of *GABRG1* and *TRAK1* mutations. *GABRG*1 p.Cys188Trp and p.Tyr178His impact conserved residues at the neurotransmitter-gated ligand binding domain of *GABRG1*. *TRAK1* p.Cys188Trp affects a conserved residue of the second kinesin-binding Milton domain. (c) Structural modeling of *GABRG1* p.Cys188Trp and p.Tyr178His mutations. p.Cys188 disulphide-bonds with Cys202. Mutation to Trp188 disrupts this conserved disulphide bond with calculated $\Delta\Delta G = 3.8$ kcal/mol. In the midst of surrounding hydrophobic residues, the side chain hydroxyl of Tyr178 hydrogen bonds with the guanidinium side chain of Arg166, stabilizing interactions between their adjacent β-sheets. Disruption of this hydrogen bond by Arg mutation to His is predicted to destabilize $\Delta\Delta G$ by 1.70 kcal/mol. (d) WT and mutant mice were examined for nocifensive withdrawal behavior following stimulation of the trigeminal nerve region in response to mechanical stimulation using a single Von Frey filament (#7; 0.6 g). The Y-axis values represent average responses to 3 stimulations (on different days; +1 = presence of a stimulus-associated grooming response; -1 = absence of grooming behavior). The Mann-Whitney test was applied to assess statistical difference between WT and mutant mice. A Kruskal-Wallis test evaluated significant differences among all sub-groups: male and female WT and mutants. P-value * < 0.05; *** < 1×10^{-3}; **** < 1×10^{-4}. (e-f) Measurement of nociceptive withdrawal threshold using the using the Simplified Up-Down method (SUDO) (Bonin et al *Mol Pain* 2014). (e) Graph showing withdrawal threshold results using an adaptation of the method to test in the region innervated by the trigeminal nerve (see Methods; Taylor et al Pain 2012). (f) Nociceptive withdrawal threshold in response to mechanical stimulation of the hind paw using calibrated Von Frey filaments. P-value ** < 0.01.

Figure 3. Gene burden analysis for heterozygous damaging mutations and mutation mapping in Ca^{2+} channels encoded by *CACNA1H* and *CACNA1F*. (a) Quantile-quantile plot of observed versus expected p-values for damaging (LoF and D-mis) variants with MAF $\leq 1x10^{-4}$. The unique genome-wide significant gene *CACNA1H* is circled in red . The genome-significance cutoff is $2.6x10^{-6}$, 0.05/19347. Mutation mapping of (b) CACNA1H and (c) CACNA1F. CACNA1H graph adapted from Rzhepetskyy et al[135]; CACNA1F graph was modified from Haeseleer et al[136].

Table 1. Demographic and clinical characteristics of TN cases and controls

REFERENCES

1. Maarbjerg S, Di Stefano G, Bendtsen L, Cruccu G. Trigeminal neuralgia - diagnosis and treatment. *Cephalalgia : an international journal of headache* **37**, 648-657 (2017).

2. Katusic S, Williams DB, Beard CM, Bergstralh EJ, Kurland LT. Epidemiology and clinical features of idiopathic trigeminal neuralgia and glossopharyngeal neuralgia: similarities and differences, Rochester, Minnesota, 1945-1984. *Neuroepidemiology* **10**, 276-281 (1991).

3. MacDonald BK, Cockerell OC, Sander JW, Shorvon SD. The incidence and lifetime prevalence of neurological disorders in a prospective community-based study in the UK. *Brain* **123 (Pt 4)**, 665-676 (2000).

4. Burchiel KJ. Abnormal impulse generation in focally demyelinated trigeminal roots. *J Neurosurg* **53**, 674-683 (1980).

5. Burchiel KJ. Ectopic impulse generation in focally demyelinated trigeminal nerve. *Exp Neurol* **69**, 423-429 (1980).

6. Devor M, Amir R, Rappaport ZH. Pathophysiology of trigeminal neuralgia: the ignition hypothesis. *Clin J Pain* **18**, 4-13 (2002).

7. Burchiel KJ, Baumann TK. Pathophysiology of trigeminal neuralgia: new evidence from a trigeminal ganglion intraoperative microneurographic recording. Case report. *J Neurosurg* **101**, 872-873 (2004).

8. Gardner Wj Fau - Miklos MV, Miklos MV. Response of trigeminal neuralgia to decompression of sensory root; discussion of cause of trigeminal neuralgia. *J Am Med Assoc* **170**, 1773-1776 (1959).

9. Hilton DA, Love S, Gradidge T, Coakham HB. Pathological findings associated with trigeminal neuralgia caused by vascular compression. *Neurosurgery* **35**, 299-303; discussion 303 (1994).

10. Rappaport ZH, Govrin-Lippmann R, Devor M. An electron-microscopic analysis of biopsy samples of the trigeminal root taken during microvascular decompressive surgery. *Stereotact Funct Neurosurg* **68**, 182-186 (1997).

11. (IHS) HCCotIHS. The International Classification of Headache Disorders, 3rd edition (beta version). *Cephalalgia* **33**, 629-808 (2013).

12. Cruccu G*, et al.* Trigeminal neuralgia: New classification and diagnostic grading for practice and research. *Neurology* **87**, 220-228 (2016).

13. Hamlyn PJ. Neurovascular relationships in the posterior cranial fossa, with special reference to trigeminal neuralgia. 1. Review of the literature and development of a new method of vascular injection-filling in cadaveric controls. *Clin Anat* **10**, 371-379 (1997).

14. Haines SJ, Jannetta PJ, Zorub DS. Microvascular relations of the trigeminal nerve. An anatomical study with clinical correlation. *J Neurosurg* **52**, 381-386 (1980).

15. Hamlyn PJ. Neurovascular relationships in the posterior cranial fossa, with special reference to trigeminal neuralgia. 2. Neurovascular compression of the trigeminal nerve in cadaveric controls and patients with trigeminal neuralgia: quantification and influence of method. *Clin Anat* **10**, 380-388 (1997).

16. Jani RH, Hughes MA, Gold MS, Branstetter BF, Ligus ZE, Sekula RF, Jr. Trigeminal Nerve Compression Without Trigeminal Neuralgia: Intraoperative vs Imaging Evidence. *Neurosurgery* **84**, 60-65 (2019).

17. Hughes MA*, et al.* Significance of degree of neurovascular compression in surgery for trigeminal neuralgia. *J Neurosurg*, 1-6 (2019).

18. Pollack IF, Jannetta PJ, Bissonette DJ. Bilateral trigeminal neuralgia: a 14-year experience with microvascular decompression. *J Neurosurg* **68**, 559-565 (1988).

19. Brisman R. Bilateral trigeminal neuralgia. *J Neurosurg* **67**, 44-48 (1987).

20. Al-Quliti KW. Update on neuropathic pain treatment for trigeminal neuralgia. The pharmacological and surgical options. *Neurosciences (Riyadh)* **20**, 107-114 (2015).

21. OL Ahmed OA, OA Akindayo, K Bamidele. Management of Trigeminal Neuralgia using Amitriptyline and Pregablin combination Therapy. *Afr J Biomed Res* **15**, 201-203 (2012).

22. Zakrzewska JM, Akram H. Neurosurgical interventions for the treatment of classical trigeminal neuralgia. *Cochrane Database Syst Rev*, CD007312 (2011).

23. Hocking LJ, Generation S, Morris AD, Dominiczak AF, Porteous DJ, Smith BH. Heritability of chronic pain in 2195 extended families. *Eur J Pain* **16**, 1053-1063 (2012).

24. Nielsen CS, Knudsen Gp Fau - Steingrimsdottir OA, Steingrimsdottir OA. Twin studies of pain. *Clin Genet* **82**, 331-340 (2012).

25. Fernandez Rodriguez B*, et al.* Familial classic trigeminal neuralgia. *Neurologia* **34**, 229-233 (2019).

26. Fleetwood IG, Innes AM, Hansen SR, Steinberg GK. Familial trigeminal neuralgia. Case report and review of the literature. *J Neurosurg* **95**, 513-517 (2001).

27. Smyth P, Greenough G, Stommel E. Familial trigeminal neuralgia: case reports and review of the literature. *Headache* **43**, 910-915 (2003).

28. El Otmani H, Moutaouakil F, Fadel H, Slassi I. [Familial trigeminal neuralgia]. *Rev Neurol (Paris)* **164**, 384-387 (2008).

29. Maarbjerg S, Wolfram F, Gozalov A, Olesen J, Bendtsen L. Significance of neurovascular contact in classical trigeminal neuralgia. *Brain* **138**, 311-319 (2015).

30. Harris W. Bilateral Trigeminal Tic: Its Association with Heredity and Disseminated Sclerosis. *Ann Surg* **103**, 161-172 (1936).

31. Cui W, Yu X Fau - Zhang H, Zhang H. The serotonin transporter gene polymorphism is associated with the susceptibility and the pain severity in idiopathic trigeminal neuralgia patients. *The journal of headache and pain* **15**, 42 (2014).

32. Tanaka BS*, et al.* A gain-of-function mutation in Nav1.6 in a case of trigeminal neuralgia. *Mol Med* **22**, 338-348 (2016).

33. Furey CG*, et al.* De Novo Mutation in Genes Regulating Neural Stem Cell Fate in Human Congenital Hydrocephalus. *Neuron* **99**, 302-314 e304 (2018).

34. Duran D*, et al.* Mutations in Chromatin Modifier and Ephrin Signaling Genes in Vein of Galen Malformation. LID - S0896-6273(18)31050-X [pii] LID - 10.1016/j.neuron.2018.11.041 [doi]. *Neuron*, (2018).

35. Iossifov I*, et al.* De novo gene disruptions in children on the autistic spectrum. *Neuron* **74**, 285-299 (2012).

36. Vissers LE*, et al.* A de novo paradigm for mental retardation. *Nat Genet* **42**, 1109-1112 (2010).

37. Allen As Fau - Berkovic SF*, et al.* De novo mutations in epileptic encephalopathies. *Nature* **501**, 217-221 (2013).

38. Jin SC*, et al.* Contribution of rare inherited and de novo variants in 2,871 congenital heart disease probands. *Nat Genet* **49**, 1593-1601 (2017).

39. Zaidi S*, et al.* De novo mutations in histone-modifying genes in congenital heart disease. *Nature* **498**, 220-223 (2013).

40. Timberlake ATA-Ohoo*, et al.* Two locus inheritance of non-syndromic midline craniosynostosis via rare SMAD6 and common BMP2 alleles. LID - 10.7554/eLife.20125 [doi] LID - e20125 [pii]. *Elife*, pii: e20125 (2016).

41. Duran D*, et al.* Mutations in Chromatin Modifier and Ephrin Signaling Genes in Vein of Galen Malformation. *Neuron* **101**, 429-443 e424 (2019).

42. Program TNT-OfPMTWGS. BRAVO variant browser.). 2018 edn. University of Michigan and NHLBI (2018).

43. Dong C*, et al.* Comparison and integration of deleteriousness prediction methods for nonsynonymous SNVs in whole exome sequencing studies. *Human molecular genetics* **24**, 2125-2137 (2015).

44. Kircher M, Witten DM, Jain P, O'Roak BJ, Cooper GM, Shendure J. A general framework for estimating the relative pathogenicity of human genetic variants. *Nat Genet* **46**, 310-315 (2014).

45. Ackerman MJ*, et al.* Postmortem molecular analysis of SCN5A defects in sudden infant death syndrome. *JAMA* **286**, 2264-2269 (2001).

46. Wei B*, et al.* Pre- and post-synaptic switches of GABA actions associated with Cl- homeostatic changes are induced in the spinal nucleus of the trigeminal nerve in a rat model of trigeminal neuropathic pain. *Neuroscience* **228**, 334-348 (2013).

47. Roberts E. GABAergic malfunction in the limbic system resulting from an aboriginal genetic defect in voltage-gated Na+-channel SCN5A is proposed to give rise to susceptibility to schizophrenia. *Adv Pharmocol* **54**, 119-145 (2006).

48. Alter BJ, Zhao C, Karim F, Landreth GE, Gereau RWt. Genetic targeting of ERK1 suggests a predominant role for ERK2 in murine pain models. *J Neurosci* **30**, 11537-11547 (2010).

49. Sun S, Sun J, Jiang W, Wang W, Ni L. Nav1.7 via Promotion of ERK in the Trigeminal Ganglion Plays an Important Role in the Induction of Pulpitis Inflammatory Pain. *BioMed research international* **2019**, 6973932 (2019).

50. Liverman CS, Brown JW, Sandhir R, Klein RM, McCarson K, Berman NE. Oestrogen increases nociception through ERK activation in the trigeminal ganglion: evidence for a peripheral mechanism of allodynia. *Cephalalgia* **29**, 520-531 (2009).

51. Eigenbrod O*, et al.* Rapid molecular evolution of pain insensitivity in multiple African rodents. *Science* **364**, 852-859 (2019).

52. Mi H*, et al.* PANTHER version 11: expanded annotation data from Gene Ontology and Reactome pathways, and data analysis tool enhancements. *Nucleic Acids Res* **45**, D183-D189 (2017).

53. Flegel C*, et al.* RNA-Seq Analysis of Human Trigeminal and Dorsal Root Ganglia with a Focus on Chemoreceptors. *PLoS One* **10**, e0128951 (2015).

54. Behesti H*, et al.* ASTN2 modulates synaptic strength by trafficking and degradation of surface proteins. *Proc Natl Acad Sci U S A* **115**, E9717-E9726 (2018).

55. Heise C*, et al.* eEF2K/eEF2 Pathway Controls the Excitation/Inhibition Balance and Susceptibility to Epileptic Seizures. *Cereb Cortex* **27**, 2226-2248 (2017).

56. Philippart F, Khaliq ZA-O. G(i/o) protein-coupled receptors in dopamine neurons inhibit the sodium leak channel NALCN. *Elife* **7**, (2018).

57. Yeh E*, et al.* A putative cation channel, NCA-1, and a novel protein, UNC-80, transmit neuronal activity in C. elegans. *PLoS Biol* **6**, e55 (2008).

58. Lyons DA, Naylor Sg Fau - Scholze A, Scholze A Fau - Talbot WS, Talbot WS. Kif1b is essential for mRNA localization in oligodendrocytes and development of myelinated axons. *Nat Genet* **41**, 854-858 (2009).

59. Aulchenko YS*, et al.* Genetic variation in the KIF1B locus influences susceptibility to multiple sclerosis. *Nat Genet* **40**, 1402-1403 (2008).

60. Zuchner S*, et al.* Mutations in the mitochondrial GTPase mitofusin 2 cause Charcot-Marie-Tooth neuropathy type 2A. *Nat Genet* **36**, 449-451 (2004).

61. Wilcox AS*, et al.* Human chromosomal localization of genes encoding the gamma 1 and gamma 2 subunits of the gamma-aminobutyric acid receptor indicates that members of this gene family are often clustered in the genome. *Proceedings of the National Academy of Sciences of the United States of America* **89**, 5857-5861 (1992).

62. Barel O*, et al.* Deleterious variants in TRAK1 disrupt mitochondrial movement and cause fatal encephalopathy. *Brain : a journal of neurology* **140**, 568-581 (2017).

63. Gilbert SL*, et al.* Trak1 mutation disrupts GABA(A) receptor homeostasis in hypertonic mice. *Nat Genet* **38**, 245-250 (2006).

64. Bailey AL, Ribeiro-da-Silva A. Transient loss of terminals from non-peptidergic nociceptive fibers in the substantia gelatinosa of spinal cord following chronic constriction injury of the sciatic nerve. *Neuroscience* **138**, 675-690 (2006).

65. Taylor AM, Osikowicz M, Ribeiro-da-Silva A. Consequences of the ablation of nonpeptidergic afferents in an animal model of trigeminal neuropathic pain. *Pain* **153**, 1311-1319 (2012).

66. Bonin RP, Bories C, De Koninck Y. A simplified up-down method (SUDO) for measuring mechanical nociception in rodents using von Frey filaments. *Mol Pain* **10**, 26 (2014).

67. Bhisitkul RB, Kocsis JD, Gordon TR, Waxman SG. Trophic influence of the distal nerve segment on GABAA receptor expression in axotomized adult sensory neurons. *Exp Neurol* **109**, 273-278 (1990).

68. Oyelese AA, Rizzo MA, Waxman SG, Kocsis JD. Differential effects of NGF and BDNF on axotomy-induced changes in GABA(A)-receptor-mediated conductance and sodium currents in cutaneous afferent neurons. *J Neurophysiol* **78**, 31-42 (1997).

69. Dieb W, Hafidi A. Mechanism of GABA involvement in post-traumatic trigeminal neuropathic pain: activation of neuronal circuitry composed of PKCgamma interneurons and pERK1/2 expressing neurons. *Eur J Pain* **19**, 85-96 (2015).

70. Jang IJ*, et al.* Acute inflammation reveals GABAA receptor-mediated nociception in mouse dorsal root ganglion neurons via PGE2 receptor 4 signaling. LID - e13178 [pii] LID - 10.14814/phy2.13178 [doi]. *Physiol Rep* **5**, (2017).

71. Martin YB, Malmierca E, Avendano C, Nunez A. Neuronal disinhibition in the trigeminal nucleus caudalis in a model of chronic neuropathic pain. *Eur J Neurosci* **32**, 399-408 (2010).

72. Kaushal R*, et al.* GABA-A receptor activity in the noradrenergic locus coeruleus drives trigeminal neuropathic pain in the rat; contribution of NAalpha1 receptors in the medial prefrontal cortex. *Neuroscience* **334**, 148-159 (2016).

73. Granger P*, et al.* Modulation of the gamma-aminobutyric acid type A receptor by the antiepileptic drugs carbamazepine and phenytoin. *Mol Pharmacol* **47**, 1189-1196 (1995).

74. White HS, Brown SD, Woodhead JH, Skeen GA, Wolf HH. Topiramate modulates GABA-evoked currents in murine cortical neurons by a nonbenzodiazepine mechanism. *Epilepsia* **41 Suppl 1**, S17-20 (2000).

75. Mousavi SH, Sekula RF, Gildengers A, Gardner P, Lunsford LD. Concomitant depression and anxiety negatively affect pain outcomes in surgically managed young patients with trigeminal neuralgia: Long-term clinical outcome. *Surg Neurol Int* **7**, 98 (2016).

76. Zimmer T, Surber R. SCN5A channelopathies--an update on mutations and mechanisms. *Prog Biophys Mol Biol* **98**, 120-136 (2008).

77. Kerr NC, Holmes FE, Wynick D. Novel isoforms of the sodium channels Nav1.8 and Nav1.5 are produced by a conserved mechanism in mouse and rat. *The Journal of biological chemistry* **279**, 24826-24833 (2004).

78. Parisi P*, et al.* Coexistence of epilepsy and Brugada syndrome in a family with SCN5A mutation. *Epilepsy Res* **105**, 415-418 (2013).

79. Souza IA, Gandini MA, Wan MM, Zamponi GW. Two heterozygous Cav3.2 channel mutations in a pediatric chronic pain patient: recording condition-dependent biophysical effects. *Pflugers Arch* **468**, 635-642 (2016).

80. Eckle VS*, et al.* Mechanisms by which a CACNA1H mutation in epilepsy patients increases seizure susceptibility. *J Physiol* **592**, 795-809 (2014).

81. Aptel H*, et al.* The Cav3.2/alpha1H T-type Ca2+ current is a molecular determinant of excitatory effects of GABA in adult sensory neurons. *Mol Cell Neurosci* **36**, 293-303 (2007).

82. Shin JB, Martinez-Salgado C, Heppenstall PA, Lewin GR. A T-type calcium channel required for normal function of a mammalian mechanoreceptor. *Nature neuroscience* **6**, 724-730 (2003).

83. Kang XJ*, et al.* Increased expression of CaV3.2 T-type calcium channels in damaged DRG neurons contributes to neuropathic pain in rats with spared nerve injury. *Mol Pain* **14**, 1744806918765808 (2018).

84. Choi S, Yu E, Hwang E, Llinas RR. Pathophysiological implication of CaV3.1 T-type Ca2+ channels in trigeminal neuropathic pain. *Proceedings of the National Academy of Sciences of the United States of America* **113**, 2270-2275 (2016).

85. An J, Wang L, Guo Q, Li L, Xia F, Zhang Z. Behavioral phenotypic properties of a natural occurring rat model of congenital stationary night blindness with Cacna1f mutation. *J Neurogenet* **26**, 363-373 (2012).

86. Revencu N*, et al.* RASA1 mutations and associated phenotypes in 68 families with capillary malformation-arteriovenous malformation. *Hum Mutat* **34**, 1632-1641 (2013).

87. Brouillard P*, et al.* Mutations in a novel factor, glomulin, are responsible for glomuvenous malformations ("glomangiomas"). *Am J Hum Genet* **70**, 866-874 (2002).

88. Pagenstecher A, Stahl S, Sure U, Felbor U. A two-hit mechanism causes cerebral cavernous malformations: complete inactivation of CCM1, CCM2 or CCM3 in affected endothelial cells. *Human molecular genetics* **18**, 911-918 (2009).

89. Gormley P Fau - Kurki MI*, et al.* Common Variant Burden Contributes to the Familial Aggregation of Migraine in 1,589 Families. *Neuron* **99**, 1098 (2018).

90. Meng W*, et al.* A genome-wide association study suggests an association of Chr8p21.3 (GFRA2) with diabetic neuropathic pain. *Eur J Pain* **19**, 392-399 (2015).

91. Meng W*, et al.* A Genome-wide Association Study Provides Evidence of Sex-specific Involvement of Chr1p35.1 (ZSCAN20-TLR12P) and Chr8p23.1 (HMGB1P46) With Diabetic Neuropathic Pain. *EBioMedicine* **2**, 1386-1393 (2015).

92. Bahgat D, Ray DK, Raslan AM, McCartney S, Burchiel KJ. Trigeminal neuralgia in young adults. *J Neurosurg* **114**, 1306-1311 (2011).

93. Zorina-Lichtenwalter K Fau - Parisien M, Parisien M Fau - Diatchenko L, Diatchenko L. Genetic studies of human neuropathic pain conditions: a review. *Pain* **159**, 583-594 (2018).

94. Haller S, Etienne L, Kovari E, Varoquaux AD, Urbach H, Becker M. Imaging of Neurovascular Compression Syndromes: Trigeminal Neuralgia, Hemifacial Spasm, Vestibular Paroxysmia, and Glossopharyngeal Neuralgia. *AJNR Am J Neuroradiol* **37**, 1384-1392 (2016).

95. Campbell E Fau - Keedy C, Keedy C. Hemifacial spasm; a note on the etiology in two cases. *J Neurosurg* **4**, 342-347 (1947).

96. Carter JB, Patrinely JR, Jankovic J, McCrary JA, 3rd, Boniuk M. Familial hemifacial spasm. *Arch Ophthalmol* **108**, 249-250 (1990).

97. Coad JE, Wirtschafter JD, Haines SJ, Heros RC, Perrone T. Familial hemifacial spasm associated with arterial compression of the facial nerve. Case report. *J Neurosurg* **74**, 290-296 (1991).

98. Friedman A, Jamrozik Z, Bojakowski J. Familial hemifacial spasm. *Mov Disord* **4**, 213-218 (1989).

99. Lagalla G, Logullo F, Di Bella P, Haghighipour R, Provinciali L. Familial hemifacial spasm and determinants of late onset. *Neurol Sci* **31**, 17-22 (2010).

100. Miwa H, Mizuno Y, Kondo T. Familial hemifacial spasm: report of cases and review of literature. *J Neurol Sci* **193**, 97-102 (2002).

101. Yekkirala AS, Roberson DP, Bean BP, Woolf CJ. Breaking barriers to novel analgesic drug development. *Nat Rev Drug Discov* **16**, 545-564 (2017).

102. Society IH. IHS Classification ICHD-3. In: *13.1.1 Trigeminal neuralgia*). International Headache Society (2018).

103. Krumm N*, et al.* Excess of rare, inherited truncating mutations in autism. *Nature genetics* **47**, 582-588 (2015).

104. McKenna A*, et al.* The Genome Analysis Toolkit: a MapReduce framework for analyzing next-generation DNA sequencing data. *Genome research* **20**, 1297-1303 (2010).

105. Van der Auwera GA, *et al.* From FastQ data to high confidence variant calls: the Genome Analysis Toolkit best practices pipeline. *Curr Protoc Bioinformatics* **43**, 11 10 11-33 (2013).

106. Genomes Project C, *et al.* A global reference for human genetic variation. *Nature* **526**, 68-74 (2015).

107. Ware JS, Samocha KE, Homsy J, Daly MJ. Interpreting de novo Variation in Human Disease Using denovolyzeR. *Curr Protoc Hum Genet*, 15 (2015).

108. Garrison E MG. Haplotype-based variant detection from short-read sequencing. *arXiv* **preprint arXiv**, [q-bio.GN] (2012).

109. Wang K, Li M, Hakonarson H. ANNOVAR: functional annotation of genetic variants from high-throughput sequencing data. *Nucleic Acids Res* **38**, e164 (2010).

110. Exome Variant Server. NHLBI GO Exome Sequencing Project (ESP).).

111. Lek M, *et al.* Analysis of protein-coding genetic variation in 60,706 humans. *Nature* **536**, 285-291 (2016).

112. Program TNT-OfPMTWGS. BRAVO variant browser: University of Michigan and NHLBI. In: *Available from:* https://bravo.sph.umich.edu/freeze5/hg38/) (2018).

113. Purcell S, *et al.* PLINK: a tool set for whole-genome association and population-based linkage analyses. *American journal of human genetics* **81**, 559-575 (2007).

114. Lek M, *et al.* Analysis of protein-coding genetic variation in 60,706 humans. *Nature* **536**, 285-291 (2016).

115. Price AL, Patterson NJ, Plenge RM, Weinblatt ME, Shadick NA, Reich D. Principal components analysis corrects for stratification in genome-wide association studies. *Nat Genet* **38**, 904-909 (2006).

116. Wang C, *et al.* Ancestry estimation and control of population stratification for sequence-based association studies. *Nature genetics* **46**, 409-415 (2014).

117. Wei Q, *et al.* A Bayesian framework for de novo mutation calling in parents-offspring trios. *Bioinformatics* **31**, 1375-1381 (2015).

118. Samocha KE, *et al.* A framework for the interpretation of de novo mutation in human disease. *Nat Genet* **46**, 944-950 (2014).

119. Raudvere U, *et al.* g:Profiler: a web server for functional enrichment analysis and conversions of gene lists (2019 update). *Nucleic Acids Res* **47**, W191-W198 (2019).

120. Ashburner M*, et al.* Gene ontology: tool for the unification of biology. The Gene Ontology Consortium. *Nat Genet* **25**, 25-29 (2000).

121. The Gene Ontology C. The Gene Ontology Resource: 20 years and still GOing strong. *Nucleic Acids Res* **47**, D330-D338 (2019).

122. Fromer M*, et al.* Discovery and statistical genotyping of copy-number variation from whole-exome sequencing depth. *American journal of human genetics* **91**, 597-607 (2012).

123. Abagyan R, Totrov M, Kuznetsov D. ICM—A new method for protein modeling and design: Applications to docking and structure prediction from the distorted native conformation. *Journal of Computational Chemistry* **15**, 488-506 (1994).

124. Pan X*, et al.* Molecular basis for pore blockade of human Na⁺ channel Na_v1.2 by the μ-conotoxin KIIIA. *Science* **363**, 1309-1313 (2019).

125. Wu J*, et al.* Structure of the voltage-gated calcium channel Ca(v)1.1 at 3.6 Å resolution. *Nature* **537**, 191-196 (2016).

126. Zhao Y*, et al.* Cryo-EM structures of apo and antagonist-bound human Ca(v)3.1. *Nature* **576**, 492-497 (2019).

127. Abagyan R, Totrov, M. Kuznetsov, D. Icm. ICM—A new method for protein modeling and design: Applications to docking and structure prediction from the distorted native conformation. *Journal of Computational Chemistry*, 18 (1994).

128. Fiser A, Sali A. Modeller: generation and refinement of homology-based protein structure models. *Methods Enzymol* **374**, 461-491 (2003).

129. Laskowski RA, MacArthur MW, Moss DS, Thornton JM. PROCHECK: a program to check the stereochemical quality of protein structures. *Journal of Applied Crystallography* **26**, 283-291 (1993).

130. Wiederstein M, Sippl MJ. ProSA-web: interactive web service for the recognition of errors in three-dimensional structures of proteins. *Nucleic Acids Res* **35**, W407-410 (2007).

131. Henao-Mejia J, Williams A, Rongvaux A, Stein J, Hughes C, Flavell RA. Generation of Genetically Modified Mice Using the CRISPR-Cas9 Genome-Editing System. *Cold Spring Harb Protoc* **2016**, pdb.prot090704 (2016).

132. Yang H, Wang H, Shivalila CS, Cheng AW, Shi L, Jaenisch R. One-step generation of mice carrying reporter and conditional alleles by CRISPR/Cas-mediated genome engineering. *Cell* **154**, 1370-1379 (2013).

133. Chang CC, Chow CC, Tellier LC, Vattikuti S, Purcell SM, Lee JJ. Second-generation PLINK: rising to the challenge of larger and richer datasets. *Gigascience* **4**, 7 (2015).

134. Yang J, Lee SH, Goddard ME, Visscher PM. GCTA: a tool for genome-wide complex trait analysis. *Am J Hum Genet* **88**, 76-82 (2011).

135. Rzhepetskyy Y, Lazniewska J, Blesneac I, Pamphlett R, Weiss N. CACNA1H missense mutations associated with amyotrophic lateral sclerosis alter Cav3.2 T-type calcium channel activity and reticular thalamic neuron firing. *Channels (Austin)* **10**, 466-477 (2016).

136. Haeseleer F, Williams B, Lee A. Characterization of C-terminal Splice Variants of Cav1.4 Ca2+ Channels in Human Retina. *The Journal of biological chemistry* **291**, 15663-15673 (2016).

Figure 1.

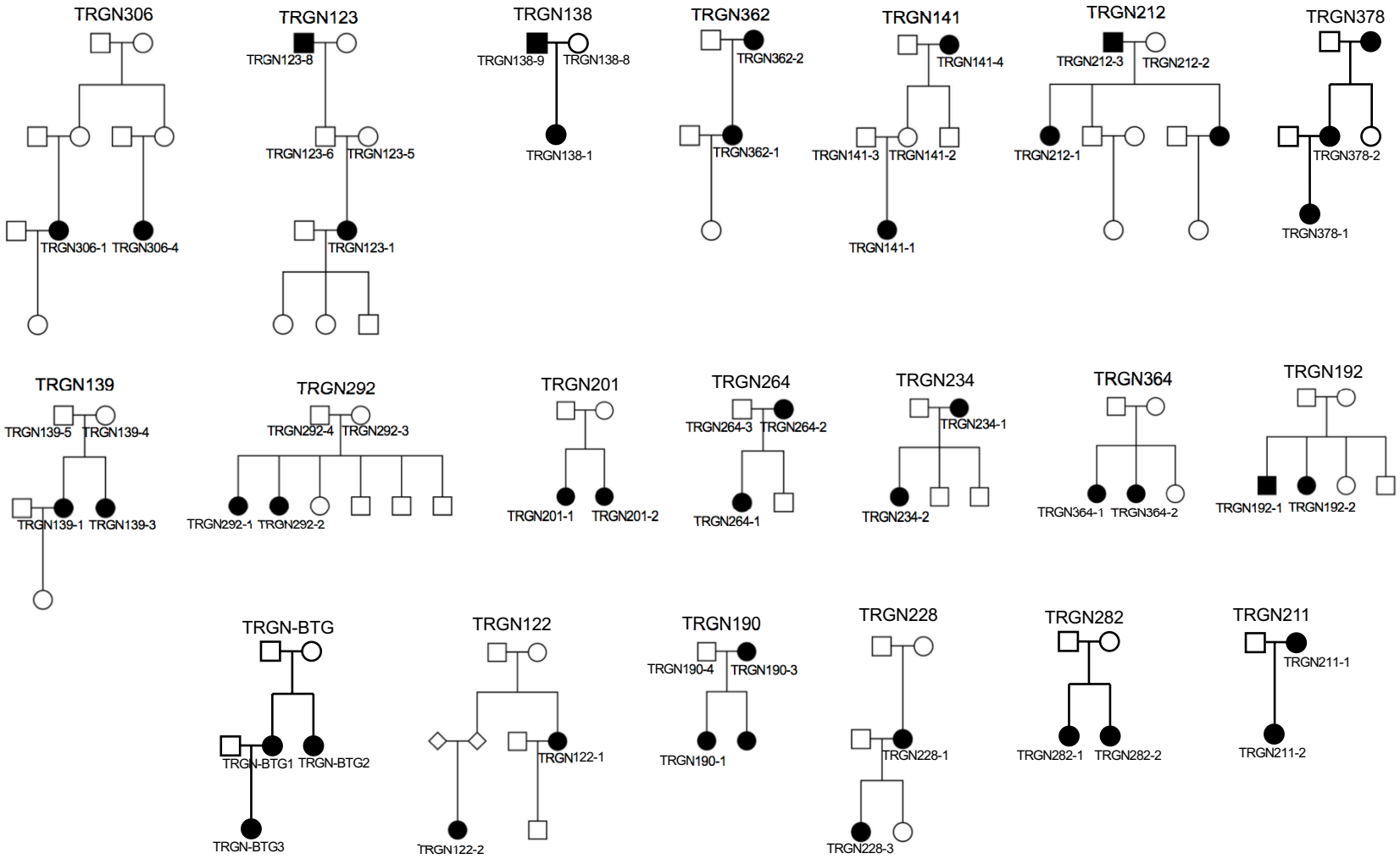
TRGN306
TRGN306-1
TRGN306-4
TRGN123
TRGN123-8
TRGN123-6
TRGN123-5
TRGN123-1
TRGN138
TRGN138-9
TRGN138-8
TRGN138-1
TRGN362
TRGN362-2
TRGN362-1
TRGN141
TRGN141-4
TRGN141-3
TRGN141-2
TRGN141-1
TRGN212
TRGN212-3
TRGN212-2
TRGN212-1
TRGN378
TRGN378-2
TRGN378-1
TRGN139
TRGN139-5
TRGN139-4
TRGN139-1
TRGN139-3
TRGN292
TRGN292-4
TRGN292-3
TRGN292-1
TRGN292-2
TRGN201
TRGN201-1
TRGN201-2
TRGN264
TRGN264-3
TRGN264-2
TRGN264-1
TRGN234
TRGN234-1
TRGN234-2
TRGN364
TRGN364-1
TRGN364-2
TRGN192
TRGN192-1
TRGN192-2
TRGN-BTG
TRGN-BTG1
TRGN-BTG2
TRGN-BTG3
TRGN122
TRGN122-1
TRGN122-2
TRGN190
TRGN190-4
TRGN190-3
TRGN190-1
TRGN228
TRGN228-1
TRGN228-3
TRGN282
TRGN282-1
TRGN282-2
TRGN211
TRGN211-1
TRGN211-2

Figure 2.

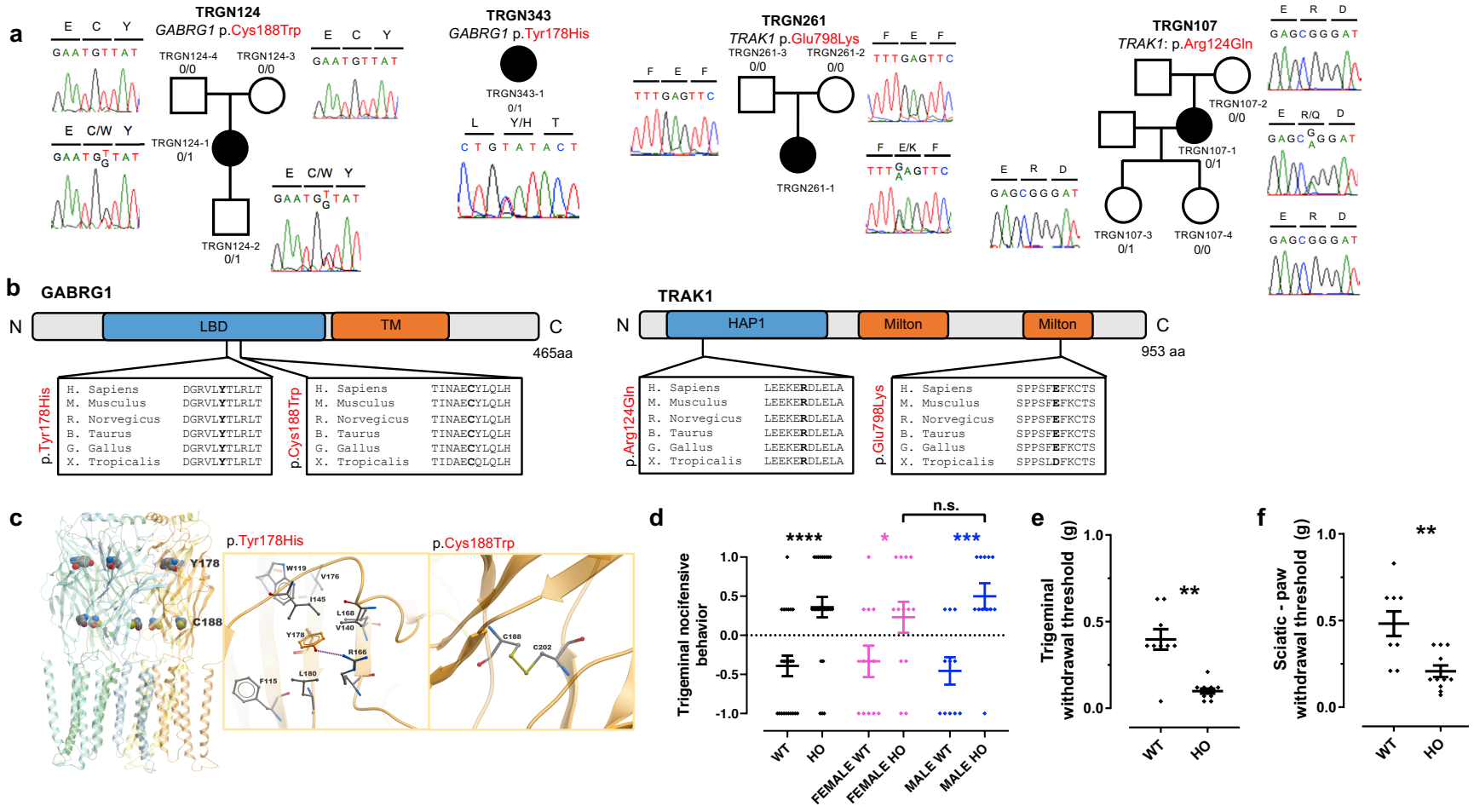
a
TRGN124
GABRG1 p.Cys188Trp
TRGN124-4 0/0
TRGN124-3 0/0
TRGN124-1 0/1
TRGN124-2 0/1
TRGN343
GABRG1 p.Tyr178His
TRGN343-1 0/1
TRGN261
TRAK1 p.Glu798Lys
TRGN261-3 0/0
TRGN261-2 0/0
TRGN261-1
TRGN107
TRAK1: p.Arg124Gln
TRGN107-2 0/0
TRGN107-1 0/1
TRGN107-3 0/1
TRGN107-4 0/0
b
GABRG1
N
LBD
TM
C
465aa
p.Tyr178His
p.Cys188Trp
H. Sapiens DGRVLYTLRLT
M. Musculus DGRVLYTLRLT
R. Norvegicus DGRVLYTLRLT
B. Taurus DGRVLYTLRLT
G. Gallus DGRVLYTLRLT
X. Tropicalis DGRVLYTLRLT
H. Sapiens TINAECYLQLH
M. Musculus TINAECYLQLH
R. Norvegicus TINAECYLQLH
B. Taurus TINAECYLQLH
G. Gallus TINAECYLQLH
X. Tropicalis TIDAECQLQLH
TRAK1
N
HAP1
Milton
Milton
C
953 aa
p.Arg124Gln
p.Glu798Lys
H. Sapiens LEEKERDLELA
M. Musculus LEEKERDLELA
R. Norvegicus LEEKERDLELA
B. Taurus LEEKERDLELA
G. Gallus LEEKERDLELA
X. Tropicalis LEEKERDLELA
H. Sapiens SPPSFEFKCTS
M. Musculus SPPSFEFKCTS
R. Norvegicus SPPSFEFKCTS
B. Taurus SPPSFEFKCTS
G. Gallus SPPSFEFKCTS
X. Tropicalis SPPSLDFKCTS
c
Y178
C188
p.Tyr178His
p.Cys188Trp
d
n.s.
Trigeminal nocifensive behavior
WT
HO
FEMALE WT
FEMALE HO
MALE WT
MALE HO
e
Trigeminal withdrawal threshold (g)
f
Sciatic - paw withdrawal threshold (g)

Figure 3.

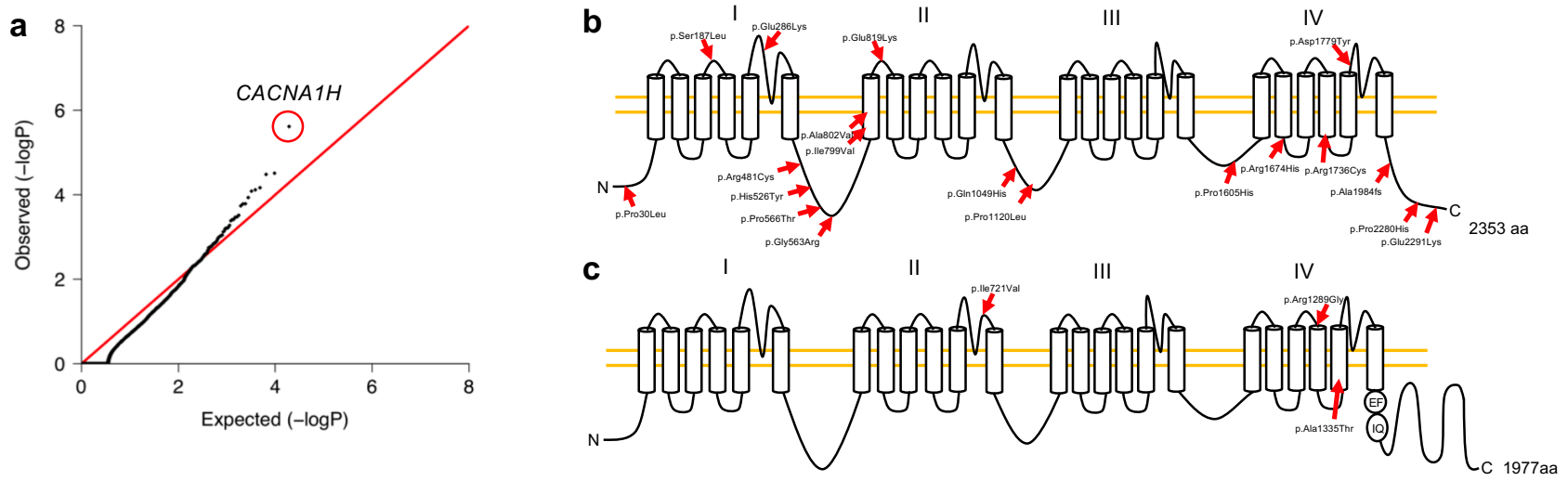
a
CACNA1H
Observed (−logP)
Expected (−logP)
0
2
4
6
8
b
I
II
III
IV
p.Ser187Leu
p.Glu286Lys
p.Glu819Lys
p.Asp1779Tyr
p.Ala802Val
p.Ile799Val
p.Arg481Cys
p.His526Tyr
p.Pro566Thr
p.Gly563Arg
p.Pro30Leu
p.Gln1049His
p.Pro1120Leu
p.Arg1674His
p.Pro1605His
p.Arg1736Cys
p.Ala1984fs
p.Pro2280His
p.Glu2291Lys
N
C
2353 aa
c
I
II
III
IV
p.Ile721Val
p.Arg1289Gly
p.Ala1335Thr
EF
IQ
N
C 1977aa

Table 1.

	TN Cases from Yale	TN Cases from UK BioBank	Autism Sibling Controls
Sample size	249	41	1,798
Trios	70 (28.1%)	0 (0.0%)	1,798 (100.0%)
Non-trio cases	179 (71.9%)	41 (100.0%)	0 (0.0%)
Cases with family history of TN	41 (16.5%)	NA	NA
Cases with ≥ 2 affected members sequenced	20 (8.0%)	NA	NA
Gender			
Male	34 (13.7%)	15 (36.6%)	842 (46.8%)
Female	215 (86.3%)	26 (63.4%)	956 (53.2%)
Ethnicity			
European	238 (95.6%)	38 (92.7%)	1,418 (78.9%)
African American	0 (0.0%)	1 (2.4%)	77 (4.3%)
East Asian	1 (0.4%)	1 (2.4%)	40 (2.2%)
South Asian	1 (0.4%)	0 (0.0%)	88 (4.9%)
Mexican	6 (2.4%)	1 (2.4%)	129 (7.2%)
Other	3 (1.2%)	0 (0.0%)	46 (2.6%)
TN type			
cTN-1	47 (18.9%)	NA	NA
cTN-2	80 (32.1%)	NA	NA
iTN-1	44 (17.7%)	NA	NA
iTN-2	78 (31.3%)	NA	NA
Bilateral symptoms	36 (14.5%)	NA	NA
Neurosurgical intervention	159 (63.9%)	NA	NA
MVD	136 (54.6%)	NA	NA
With relief of symptoms	75 (30.1%)	NA	NA
No relief of symptoms	58 (23.3%)	NA	NA
Repeated MVD	26 (10.4%)	NA	NA
Thermal or balloon rhizotomy	29 (11.6%)	NA	NA
Gamma knife	37 (14.9%)	NA	NA
Other	22 (8.8%)	NA	NA

The number of samples is shown in each category with the corresponding percentage in parentheses. Some Trios contain ≥ 2 affected members. Ethnicity is determined by principal component analysis compared to HapMap samples using EIGENSTRAT.